Ice thickness measurements in Lake Erie during the winter of 2010-2011

Nathan Hawley[a,*], Dmitry Beletsky[b], Jia Wang[a]

[a] Great Lakes Environmental Research Laboratory, 4840 S. State Road, Ann Arbor, MI 48108, USA,

[b] Cooperative Institute for Great Lakes Research, University of Michigan, 4840 S. State Road, Ann Arbor, MI 48108

Corresponding author: nathan.hawley@noaa.gov,734-741-2273, 734-741-2055 (fax),

Abstract:

Time series measurements of ice thicknesses were made at either 1 or 2 Hz at 6 locations in the western part of Lake Erie's central basin during the winter of 2010-2011. Ice was observed over approximately 80 days beginning in late December and continuing through mid-March. Deformation and ridging of ice occurred frequently and produced ice thicknesses of up to 10 m, and over 6 m at all stations. The measurements show considerable variability (up to several meters) between stations, even when the distance between them is less than 500 m. Comparison of the measurements to those generated by the National Ice Center show good agreement for undeformed thicknesses, but the Ice Center analyses do not account for increased thicknesses due to ice ridging. Several different measures of ice thickness (based on different averaging times and the parameter used to characterize the resulting distribution of thicknesses) are used to characterize the data, and the results can vary widely depending upon which measure is used. The best measure to use will depend upon the use for which the data is intended.

key words: ice thickness, Lake Erie, ice ridge

Introduction

The presence of wide-spread ice cover on the Laurentian Great Lakes significantly influences lake-effect snow/storms (Notaro et al. 2013), regional weather, the hydrological cycle, water levels, water temperature (Wang et al. 2010), and the circulation of the lakes (Fujisaki-Manome et al. 2013). Knowledge of the growth and decay rates of ice are also needed for models of the thermal cycle of the lakes as well as for navigation and recreational purposes. Although the importance of ice measurements is well known, logistical difficulties make direct observations, particularly of ice thickness, quite rare. When these measurements are made, they are usually point measurements made with an ice auger. Titze and Austin (2016) reported observations of ice movement in Lake Superior during the winter of 2013-2014 and summarized previous work on ice in the Great Lakes. As they noted, ' …literature addressing ice on the Laurentian Great Lakes focuses almost entirely on remotely sensed data … or modeling studies.' Titze and Austin (2016) used acoustic current profilers to measure ice transport and reported ice thicknesses measured when the passage of ice keels changed the depth recorded by subsurface pressure sensors. At one station (where the pressure sensor was approximately 5 m below the surface), they report frequent thicknesses of 5-8 m, and one instance of a keel 11 m thick. At each of two other stations (where the pressure sensor was located about 13 m below the surface), they found at least one instance of keels greater than 12m thick. To our knowledge, these are the only *in situ* time series measurements of ice properties in the Laurentian Great Lakes.

Ice in the Great Lakes is seasonal ice. In most areas it is not frozen to the shoreline, and typically has thicknesses ranging from a few centimeters to one meter or more. Ice usually begins to form in the Great Lakes in December and January and reaches its maximum extent in February or early March (Wang et al. 2012). Ice cover can be very transitory, particularly in the

mid-lake areas, where lake heat storage, air temperature, and wind can move, compact, and alter the concentration and thickness of the ice cover. There is also significant inter-annual variability (Bai et al. 2012). Leppäranta (2015) and Kirillin et al. (2012) reviewed the characteristics and behavior of ice in freshwater lakes, but most of the observations were made on lakes much smaller than the Laurentian Great Lakes.

Lake Erie is the smallest of the Great Lakes by volume, and is divided into three basins. Our measurements were made in the central basin of the lake, which is approximately 70-100 km wide and about 180 km long with a maximum depth of 25 m. This makes it a large, shallow lake according to the classification of Leppäranta (2015). The large size of the basin means that wind-generated waves can be significant mixing agents, while its shallow depth means that freezing occurs during most winters.

In Lake Erie, the spatial progression of ice formation is from the shallow west basin (maximum depth 10 m) in late December to the deeper central (maximum depth 25 m) and eastern (maximum depth 64 m) basins in January. In the central basin, new ice forms on the northern shore first. Lake Erie reaches its maximum ice cover by the end of January and retains this cover through February (Assel 1990). While providing the greatest probability of extensive ice cover, this period also often features large variability in ice concentration (Assel, R.A. 2003. An electronic atlas of Great Lakes ice cover, *NOAA Great Lakes Ice Atlas*, NOAA Great Lakes Environmental Research Laboratory, Ann Arbor, MI., www.glerl.noaa.gov/data/ice/atlas, accessed December 8, 2017).

Analysis of ice cover and thickness in the Great Lakes is conducted jointly by the National Ice Center in the USA and the Canadian Ice Center. Satellite imagery is analyzed to determine the

ice cover and combined with estimates of the ice thickness determined by a degree-day model. A chart is published at least once a week and more often when changes occur quickly.

This study documents *in situ* time series measurements of ice thickness made in the central basin of the lake during the winter of 2010-2011 as part of a joint NSF-NOAA program to measure and model ice growth and its effects in Lake Erie. The ice cover in Lake Erie during the winter of 2010-2011 was above average but not atypical; Assel et al. (2013) found that the maximum ice cover in Lake Erie in 2010-2011 was the 10th highest out of the 39 years between 1973 and 2011.

Methods

Instrumented moorings were deployed at 7 locations in the central basin of Lake Erie in the fall of 2010 and retrieved in the spring of 2011 (Fig. 1). Details of the instruments deployed at each station are given in Table 1. Elevations in the table are in meters above bottom (mab). Different combinations of sensors were deployed on two separate moorings at each station. At stations 1-4, a SWIPS ice profiler manufactured by ASL Environmental Sciences and 4 to 6 Sea Bird 39 temperature sensors were mounted at either end of a 50 m ground line that was anchored with a concrete weight at both ends. A separate mooring contained either an RDI ADCP (at stations 1-3) or a Nortek AWAC current profiler. At stations 5-7 a bottom–resting tripod was deployed on one mooring, and the temperature sensors and either an RDI ADCP (at station 7) or a Nortek AWAC profiler were on the other. The tripods were instrumented with Sea Tech transmissometers and Paroscientific pressure sensors. Previous experience in Lake Erie in 1979-1980 showed that ice thicknesses could reach up to 10 m during the spring (G. Miller, personal communication), so all sensors were located at least 10 m below the water surface.

SWIPS ice profilers manufactured by ASL Environmental Sciences were deployed to measure ice thickness at stations 1-4. These profilers emit a single vertical acoustic beam at 546 kHz to measure the range to the bottom of any ice present. The instruments were mounted on a mooring 2-3 mab supported by subsurface floats. Between December 12 and May 1 the instruments were configured to make range measurements each second, and measurements of water pressure, water temperature, pitch, and roll every 10 seconds.

Acoustic current profilers were deployed at all 7 stations. At stations 1, 2, 3, and 7, upward looking RDI ADCPs were deployed at 0.5 mab. Currents were sampled in 1 m bins every 10 minutes. All the ADCPs also included RDI's ice-tracking software to track the velocity of any ice present. At stations 4, 5, and 6 upward-looking Nortek AWAC profilers were deployed at 0.5 mab. Currents were sampled in 1 m bins for 5 minutes every 30 minutes. These units also have a vertical acoustic beam to measure the range to the bottom of any ice present. Burst observations of the range, ice velocity, and pressure were made at 1 Hz for 1024 observations every hour. These stations are designated as stations 4a, 5a, and 6a in the remainder of this manuscript.

Hourly observations of air temperature, air pressure, wind speed, and wind direction were obtained from the National Weather Service Station located at Burke Airport located along Cleveland's lakefront. MODIS images of the ice cover in the lake were obtained from NOAA's CoastWatch program. Although cloud cover masks the lake surface for much of the observation period, clear images of the central basin were obtained about once per week.

The theory for calculating the ice thickness from the *in situ* observations is straight forward. Acoustic measurements of the range from the instrument to the bottom of the ice are subtracted

from the total pressure measured by a pressure sensor to determine the thickness of the ice. This procedure does not distinguish between the contributions to the pressure measurement of ice and any snow present, and unless a separate measurement of the snow thickness and density is made, the two cannot be separated. In this study the effects of snow are probably small (D. Fissel, personal communication). Even if the effects of snow are neglected, the calculation is complicated since corrections for atmospheric pressure, instrument tilt (which affects range measurements), and changes in the speed of sound (which affects the range measurements and is affected by water temperature and salinity) all need to be included. For the SWIPS ice profilers the manufacturer has written a library of Matlab subroutines to aid in the processing; their use is documented in the IPS Processing Toolbox Users Guide (ASL Environmental Sciences, 2011). The process is an iterative one, and one of the keys is to identify periods when there is no ice cover and use those measurements to correct the other measurements. Fortunately, there were numerous such episodes at each station during the deployments described here. ASL Environmental Sciences states that the minimum ice thickness that can be measured is 0.05 m. For these deployments, the process produced a time series of ice thickness measurements every second. These were then averaged over 1 minute, 10 minute and 60 minute intervals.

The procedure used to calculate the ice thickness from the Nortek AWAC data is similar but varies slightly because of the sampling differences. The Nortek procedures are documented in Lohrmann et al. (2010) and Magnell et al. (2010), who state that the resolution is 0.05 m. Because the AWAC measurements were made in 17 minute bursts each hour, rather than continuously, the observations were averaged into hourly burst averages.

Significant wave height, peak-energy wave period, and dominant wave direction were calculated from the AWAC measurements using Nortek's Storm software. Significant wave height and

peak-energy wave period were calculated from the pressure measurements made at stations 5, 6, and 7 using the method described by Hawley et al. (2004).

Results

Satellite and meteorological observations

MODIS images show that ice began to form in the central basin in late December and that the coverage was virtually complete by late January. The cover was not continuous however, as evidenced by the cracks between the floes (Fig. 2). Ice cover was present over the entire observation area through early February, then decreased until about February 22. Ice cover increased again later in the month and in early March before it decreased again as the spring thaw began. After March 12 little or no ice was observed in the deployment area. We limit our discussion in the rest of the paper to the 80 day period between December 26, 2010 and March 16, 2011.

Meteorological observations (Fig. 3) show that beginning on about January 5 the air temperature was generally below freezing until February 9. It was usually above freezing until about February 21, decreased below freezing until about February 26, and then was usually above freezing until the end of the ice cover period. Water temperatures were essentially isothermal at all stations and reached 0° C from mid-January until mid-February. They rose slightly for about 10 days, and then were near 0° C until mid-March. These changes in air and water temperature agreed quite well with the observed changes in ice cover. The wind speeds frequently exceeded 10 m s^{-1}, which is sufficient to generate relatively large waves (wave heights > 1m) in the central basin during ice-free conditions (Hawley and Eadie, 2007). At station 7 (co-located with Hawley and Eadie's station at the deepest point in the central basin) significant wave heights exceeded 1

m numerous times, but there are no instances of large waves from January 13 to February 14 or after February 20 until March 16, even though wind speeds were just as high as during the periods when large waves did occur. These data are consistent with the satellite observations of extensive ice cover, which would inhibit wave formation. Note that since these observations were made with a pressure sensor located about 24 m below the water surface, any signal from waves with periods of less than 5.5 s would be negligible because of the attenuation of wave action with depth, but wave heights computed by Great Lakes Coastal Forecast System show similar results, with wave heights less than 0.1 m during much of the deployment.

SWIPS measures of ice thickness

Given the high frequency of the ice measurements a way to characterize the ice thicknesses is needed so that the measurements can be used as input to computer models and interpreted in a meaningful way. Fig. 4 shows ice measurements made at station 1 on February 3, 2011. The satellite imagery shown in Fig. 2 was taken at 1600 on this date. Fig. 4a shows the thicknesses calculated each second. There is considerable short-term variability in these data so, as a first step, the data were averaged at 1, 10, and 60 minute intervals (Figs. 4b, 4c, and 4d). All three averages show the same general pattern, but averaging the data, particularly over 10 and 60 minutes, significantly decreases the maximum thicknesses. The standard deviations are relatively small for all three averages. The most obvious feature of the observations is the large variability with ice thicknesses ranging between 0.1 to over 2m over periods of minutes to hours. This temporal variability is undoubtedly due to lateral variations in the ice thickness as it is transported over the sensor. Another obvious feature of the observations is the period between hours 3 and 12 when the thickness is consistently small, but not zero. Similar intervals occur

almost every day at all of the stations (although not always for as long a period), and provide a good measure of the undeformed ice thickness.

Given the temporal variability in the data and the effects of averaging, it is important to determine whether or not simply averaging the data is useful, or whether other measures of the ice thickness may be more informative. Figure 5a shows the distribution of ice thicknesses of the 1 minute, 10 minute and 60 minute averages at station 1 on February 3. All three averages show that the vast majority of the observations are less than 0.5 m, with a long tail of thicker measurements due to ice ridging. These distributions are similar to those found in the Arctic and Antarctic oceans (Hass, 2017). Both the 1 minute and 10 minute averages have a large peak at 0.2 m, but the hourly averages are bimodal, with peaks at 0.1 and 0.4 m. This is undoubtedly an artifact of the averaging. These data can be shown more compactly by calculating the cumulative distribution of the thicknesses that are greater than a given percentage of the observations. These percentiles (calculated at 10% intervals) for Feb. 3 based on the 1 minute, 10 minute, and hourly averages are shown in Fig. 5b. The percentiles are quite similar up to the 90^{th} percentile—after that they diverge widely since the maximum values are so different (Fig. 4). The data also show that the increase in thickness between the 10^{th} and 80^{th} percentiles is fairly small (less than 0.5m) for all three data sets. These trends are seen in many of the daily results, although not all are as uniform as the data shown here (the 90^{th} percentiles frequently diverge considerably more than those shown here), and there are some days where the distribution of the thicknesses is quite different. Nevertheless, it seems as though the 10^{th} percentile is a reasonable measure of the undeformed thickness, while the 80^{th} percentile seems

to be a good measure of the deformed thickness. Unless stated otherwise, the 10th and 80th percentiles calculated from the 10 minute averages are used in the remainder of the paper.

Temporal and spatial variability of the SWIPS measurements

The 10 minute averages and the 10th and 80th percentiles (based on the 10 minute averages) at stations 1-4 (these are the stations where SWIPS profilers were deployed) are shown in Figure 6. The averages (Figs. 6a and 6b) are quite noisy, and although all four stations show similar temporal trends, there are large differences between the stations. These differences are more easily seen in the 10th and 80th percentile data shown in Figs. 6c and 6d. The 10th percentile data at station 1 show that ice occurs at this station several days before it occurs at the other stations, and the peak thicknesses are considerably greater. Otherwise the thickness (once ice forms) at all of the stations ranges from about 0.1 to 0.25 m throughout the deployment, with the greatest thicknesses at station 4. Thicknesses at stations 2 and 3 are similar to each other and are usually less than 0.2 m.

The 80th percentile data shows the same peak at station 1, but peaks occur several times at station 4, and at station 2 near the end of the deployment. Both the 10th and 80th percentiles at station 3 (the northernmost on the western transect, Fig. 1), are consistently lower than those at the other stations. The large peaks at stations 1 and 4 are almost certainly due to ice ridging; the satellite images show frequent occurrences of ice piling up along the southern shore of the lake. During such episodes the 10th and 80th percentiles may not be appropriate measures to use to characterize the thickness and the original data will have to be examined in more detail.

AWAC ice measurements

Ice measurements were also made using Nortek AWAC sensors at stations 4, 5 and 6. To distinguish these measurements from the SWIPS measurements, the AWACS measurements are labeled as stations 4a, 5a, and 6a. Because the measurements were made in bursts (1024 observations measured at 1 Hz each hour), rather than continuously, only the burst averages of ice thickness are used. Fig 7 shows the burst averages, and the 10^{th} and 80^{th} percentiles for the three stations. The results are similar to those at stations 1-4 (Fig 6), although the thicknesses are somewhat less. A more detailed comparison of results between the two sensors can be made at station 4, where both an AWAC and a SWIPS sensor were deployed. Fig 8 shows the average thickness, and the 10^{th} and 80^{th} percentiles at this station for the two sensors. (Note that for this comparison, the SWIPS data were recalculated as burst averages of 1024 observations per hour so that the sampling was the same). Although the 10^{th} percentile data looks quite similar, both the averaged data, and the 80^{th} percentile data show distinct differences. In particular, the SWIPS data shows peaks when the AWAC sensor does not, while the AWAC sensor shows a peak on March 8 that is much larger than that recorded by the SWIPS sensor. A direct comparison of the two measurements (Fig 9) shows considerable scatter, but no systematic trend. Magnell et al. (2010) reported good agreement between the two types of sensors for a similar comparison, but their measurements were done on fast ice, and the distance between the sensors is not given. Because the two sensors in this case were located about 400 m apart, the differences are probably primarily due to real changes in ice thickness over this distance.

Discussion

The high variability of the observations means that there is no obvious coherence in the observations at different stations. Nor is there any obvious correlation between the thicknesses and the wind stress. However, the observations can be compared to other estimates of the ice thickness.

Comparison to other estimates of ice thickness

No independent measurements of ice thickness were made in Lake Erie during this winter, but the National Ice Center (NIC) published ice analyses for Lake Erie on more than 40 days during the ice season. These analyses are based on remote sensing observations coupled with a degree-day model to estimate the ice thicknesses. The analyses report the concentration of ice in 10% intervals for 5 thickness ranges: 0-0.05 m, 0.05-0.15m, 0.15-0.30 m, 0.30-0.70 m, and greater than 0.70 m (no observations of ice this thick were reported from Lake Erie). A sample of these results is shown in Table 2, where the estimates for February 3, 2011 are compared to the thicknesses reported here (Table 3). On this day, all of the stations reported here were in one of two areas reported by the NIC—one (section J) located along the south shore of the lake centered near Cleveland that included stations 1, 4, 4a, and 5a, and a second (section G) that covered the remainder of the area encompassed by the stations. The total ice cover in both sections was 100%. In section J, 70% of the ice was estimated to be 0.15-0.30 m thick and 30% between 0.30-0.70 m. In section G, the ice was somewhat thinner with 30% between 0.05-0.15 m and 70% between 0.15-0.30 m. The daily means for all stations in section J are within the ranges reported by the NIC and the 10^{th} and 80^{th} percentiles (calculated from the hourly and burst averages) are either within or are very close to the NIC range, except at station 4, where the 80^{th} percentile is somewhat above the upper limit of the NIC range. The results for section G are somewhat different. All of the means are above the upper limit of the NIC range and the 10^{th}

percentiles fall roughly in the middle of the NIC range. This is shown more clearly in Figs. 10 and 11, which compare the hourly and 10 minute average thicknesses to the NIC data. These figures show that the thicknesses reported here are frequently much greater than those reported by the NIC, and that these greater thicknesses occur frequently. This is not surprising since the NIC analysis does not take ridging into account. However, the NIC thicknesses appear to be a good estimate of the undeformed thickness.

In Table 4 the mean difference between the NIC results and the percentiles calculated from the time series observations at each station are shown Results are presented for the 4 thickness intervals for each day when the NIC reported greater than 10% ice cover. A positive number indicates that the percentage calculated from the time series measurements was greater than the NIC result, while a negative number indicates the reverse. The results show that the thicknesses calculated from the time series observations are almost always greater than those reported by the NIC. These differences vary considerably both at a given station and for a given thickness range. There is a considerable difference between the results at stations 4 and 4a, which were only a few hundred meters apart. The standard deviations of these differences are also large (Table 5), so it is hard to say anything more about these results, other than that the time series measurements in general give greater thicknesses than the NIC analyses. What is clear is that the time series observations show both considerable variability over short time intervals at all of the stations, and that the ice thicknesses are frequently considerably larger than those reported by the NIC, with thicknesses frequently greater than 1 m at all of the stations, and thicknesses greater than 5 m not uncommon. Estimation of the maximum thicknesses is best determined using the 1 minute averages. Table 6 shows the maximum ice thicknesses recorded at all of the stations (for this table, the 1 minute averages recorded during each burst at stations 4a, 5a, and 6a were

computed). The data clearly show the decrease in thickness with increasing averaging time, and they also show that even if the daily averages are used, the maximum thickness at all but station 3 is over 1 m. The maximum 1 minute averages range from about 6-10 m. It is unclear what the relationship between the maximum thickness of fresh water ice and the undeformed thickness is; but for salt water ice, Amundrud et al. (2004) developed an empirical relationship for the maximum ice thickness of sea ice

$$h_{max} = 20*h^{0.5} \quad (1)$$

where h_{max} is the maximum thickness and h is the undeformed ice thickness. For maximum thicknesses of 6-10 m, this gives values of m of 0.09-0.25 m, which are well within the undeformed ice thicknesses (as measured by the 10^{th} percentile).

Both the maximum thicknesses and their short-term variability are also similar to observations made both using acoustic ice profilers in other settings (Bjork et al., 2008; Belliveau et al. 2001; Chave et. al. 2004; and Magnell et al. 2010) and helicopter surveys of ice thickness. Although not directly comparable (because the profilers measure the change in time at a single point while helicopter surveys measure the change in space at a single time), ice thicknesses measured by electromagnetic measurements mounted on helicopters show similar variations in thickness over distances of several hundred meters in both the Arctic and Antarctic (summarized in Haas, 2017). If one assumes an average ice velocity of 0.08 m/s (Campbell et al. 1987), then ice would move about 300 m/hour. Variations on this scale in the data reported by Haas are similar to the hourly data shown here. These other observations, plus those reported by Titze and Austin

(2016) from Lake Superior, all suggest that the results reported here are similar to those made in other locations.

First ice occurrence

Determining when ice first forms from the observations is relatively easy, but not necessarily accurate, since ice thicknesses less than 0.05 m cannot be identified Fig 6 shows that ice is first observed at stations 1-3 between December 28 and January 1, followed by a period of several days when little or no ice is observed. Ice analyses from the National Ice Center show a similar pattern, with an extension of ice eastward to stations 1, 2, and 3 from the western basin between December 27-30, followed by a retreat of the ice between December 31 and January 6. At all three stations, the thicknesses are up to 2 m thick, which is possible if non-deformed ice thicknesses are at least 0.03m (Equation 1). No notable ice is observed at stations 4, 5, and 6 until about mid-January (Figs. 6 and 7), which is also consistent with the NIC ice analyses. For thermal models, a daily average may be good enough.

The results show that different measures of ice thickness can be used to characterize the observations, and that the most appropriate measure to use depends upon the use for which it is intended. For the comparison to the ice center thicknesses, the 10^{th} percentile of the daily ice distributions were used, but for other ice models another parameter may be more appropriate for model verification (depending upon the model output, time step and grid size). The model used by Fujisaki-Manome et al. (2013), for instance, calculates an ice thickness distribution at each point on a 2 km grid. Assuming an ice velocity of 0.05-0.1m per second it would take 5-10 hours for transport between grid points, so the daily ice thickness distributions would be the best data for comparison. For calculations of ice transport from observations, 10 minute or hourly

averages may be more useful, depending upon the frequency of the velocity measurements. The 1 minute averages best represent the variability of the observations and would be the best measure when determining the maximum thicknesses or the amount of ice ridging.

Conclusions

Ice thicknesses in the Lake Erie can vary considerably (by up to several meters) both with time and location. In this regard the behavior of the ice is similar to that in the oceanic marginal ice zone in that the ice cover varies widely over short distances and responds rapidly to changing weather conditions. There is no obvious coherence in the observations at the different stations, nor is there any obvious correlation with the wind stress. Estimates of the thickness by two different sensors vary considerably, but this variation is probably due to the distance between the sensors. When these measurements are compared to the ice thicknesses calculated by the National Ice Center, there is good agreement for the undeformed thicknesses, but the data reported here clearly show that deformed ice occurs frequently, with thicknesses often exceeding several meters. The high variability in the measurements makes it difficult to determine a single meaningful thickness; most likely the thickness to be used will depend upon the purpose for which it is needed. Even using hourly averages, the time series of ice thicknesses show that significant ice ridging occurs and that this process frequently produces thicknesses of 1-2 m, compared to undeformed ice thicknesses of 0.10-0.25 m. Thus these processes need to be incorporated into the present lake ice models for the Laurentian Great Lakes.

Acknowledgments: Sincere thanks to the crew of the RV Laurentian for assisting with the deployment and retrieval of the moorings, and to the technicians in the Marine Instrumentation Laboratory at the Great Lakes Environmental Research Laboratory for preparing the instruments. Thanks also to David Fissel and the staff at ASL Environmental Sciences and to Eric Siegel and the staff at Nortek USA for encouragement and advice in processing the data. The comments of Jay Austin and two anonymous reviewers considerably improved the manuscript. This research was partially funded by NSF Grant OCE 0927643 to Dmitry Beletsky. This is NOAA GLERL contribution number xxxx and CIGLR contribution # 1121.

References

Amundrud, T. L., Melling, H., Ingram, R.G., 2004. Geometrical constraints on the evolution of ridged sea ice, J. Geophys. Res., 109, doi: 10.1029/2003JC002251.

ASL. 2011. IPS Processing Toolbox User's Guide, ASL Environmental Sciences, Sidney, British Columbia, Canada.

Assel, R.A., 1990. An ice-cover climatology for Lake Erie and Lake Superior for the winter seasons 1897–98 to 1982–83, Int. J. Climatol., 10, 731–748.

Assel, R.A., J. Wang, A.H. Clites, and X. Bai, 2011. Analysis of Great Lakes ice cover climatology: winters 2006-2011. NOAA Technical Memorandum GLERL-157, 26pp.

Bai, X., Wang, J., Sellinger, C.A., Clites, A. H., Assell, R.A., 2012. Interannual variability of Great Lakes ice cover and its relationship to NAO and ENSO. J. Geophys. Res.,

doi:10.1029/2010JC006932 .

Belliveau, D.J., Hayden, H., Prinsenberg, S., 2001. Ice drift and draft measurements from moorings at the Confederation Bridge, Proc. of the 16th International Conf. on Port and Ocean Engineering under Arctic Conditions, Port and Ocean Engineering under Arctic Conditions, 349-358.

Bjork, G., Nohr, C., Gustafsson, B.G., Lindberg, A.E.,. 2008. Ice dynamics in the Bothnian Bay inferred from ADCP measurements, Tellus 60a, 178-188.

Campbell, J. A., Clites, A.H., Greene, G.M., 1987. Measurements of ice motion in Lake Erie using satellite-tracked drifter buoys, NOAA Data Report ERL GLERL-30, Ann Arbor, MI, 20 pp.

Chave, R.A.J., Lemon, D.D., Fissel, D.B., Dupuis, L., Dumont, S., 2004. Real-time measurements of ice draft and velocity in the St. Lawrence River, Proc. Oceans 2004, MTS/IEEE, 1629-1633.

Fujisaki-Manome, A., Wang, J., Bai, X., Leshkevich, G., Lofgren. B., 2013. Model-simulated interannual variability of Lake Erie ice cover, circulation, and thermal structure in response to atmospheric forcing, 2003–2012, J. Geophys. Res. Oceans, 118, doi:10.1002/jgrc.20312.

Haas, C., 2017, Sea ice thickness distribution, in: Thomas, D.V. (Ed.), Sea Ice, John Wiley and Sons LTD, Bognor Regis, Great Britain, pp. 42-64.

Hawley, N., Eadie, B.J., 2007. Observations of sediment transport in Lake Erie during the winter of 2004-2005, Jl. Great Lakes Res. 33, 816-827.

Hawley, N., B.M. Lesht, and D.J. Schwab. 2004., A comparison of observed and modeled surface waves in southern Lake Michigan and the implications for models of sediment transport, Jl. Geophysical Res., 109, doi: 10.1029/2002JC001592.

Kirillin, G., Leppäranta, M., Terzhevik, A., Granin, N., Bernhardt, J., Englehardt, C., Efremova, T., Golosov, S., Palshin, N., Shertstyankin, P., Zdorovennova, G., Zdorovennov, R., 2012. Physics of seasonally ice-covered lakes: a review, Aquatic Sciences, 74, 659-682, doi. 10.1007/s00027-012-0279-7.

Leppäranta, M. 2015. Freezing of lakes and the evolution of their ice cover, Springer, Berlin, 301 pp.

Lohrmann, A., Pedersen, T., Nylund, S., Siegel, E., 2010. Waves in the summer, ice in the winter, Proc. IEEE/OES/CWTM tenth working conference on current measurement technology, 150-158..

Magnell, B., Ivanov, L., Siegel, E., 2010., Measurements of ice parameters in the Beaufort Sea using the Nortek AWAC acoustic doppler current profiler, Proceedings, Oceans 2010, Marine Technological Society, doi 10.1109/Oceans.2010.566416.

Notaro, M., Holman, K.A., Zarrin, E., Fluck, S., Vavrus, S., Bennington, V., 2013. Influence of the Laurentian Great Lakes on regional climate, J. Clim., 26, 789–804.

Prinsenberg, S.J., Peterson, I.K., 2001. Pack ice thickness and concentration measurements from the area around the Confederation Bridge (Canada) using helicopter-borne sensors, Proc. of the 16th International Conference on Port and Ocean Engineering under arctic conditions, Port and Ocean Engineering under Arctic Conditions, 339-348.

Prinsenberg, S.J., Van der Baaren, A., Peterson, J.K.,. 2006. Ice ridging and ice drift in southern Gulf of St. Lawrence, Canada, during winter storms, Annals of Glaciology, 44, 411-417.

Titze, D., Austin, J., 2016. Novel, direct observations of ice on Lake Superior during the high ice coverage of winter 2013-2014, J. Great Lakes Res., 42, 997-1006.

Wang, J., Hu, H., Schwab, D.J., Leshkevich, G., Beletsky, D., Hawley, N., Clites, A.H., 2010, Development of the Great Lakes Ice-circulation Model (GLIM): Application to Lake Erie in 2003-2004. Journal of Great Lakes Research, 36, 425-436, doi: 10.1016/j.jglr.2010.04.002

Wang, J., Bai, X., Hu, H., Clites, A.H.,Colton, M., and Lofgren, D., 2012. Temporal and spatial variability of Great Lakes ice cover, 1973-2010. J. Climate, doi: 10.1175/2011JCL14066.1

Figure captions

Figure 1. Mooring locations. Dotted lines show bathymetry contours at 10 m intervals.

Figure 2. MODIS imagery at 1600 UTC on February 3, 2011. Station locations shown in Figure 1 are marked by the dots.

Figure 3. A: Air temperatures at Cleveland. B: Water temperatures at station 1 measured 2 mab (dotted line) and 8 mab (solid line). The water was isothermal after January 1. C. Wind speed at Cleveland. D: Significant wave height at station 7. Because these measurements were made with a pressure sensor located about 24 m below the surface, only the effects of waves with periods greater than 5.5 s were recorded. This means that the recorded wave heights were equal to zero during much of the deployment.

Figure 4. Ice thicknesses measured at station 1 on February 3, 2011. A. One second observations. B. One minute averages and standard deviations. C. Ten minute averages and standard deviations. D. Hourly averages and standard deviations. Note that the vertical axis in panels A and B is different than that in panels C and D. The time of the MODIS image in Fig. 2 is indicated by the X in each panel.

Figure 5. A. Ice thicknesses at station 1 on February 3 for the 1 minute, ten minute, and hourly averages. The frequencies are presented as the fraction of the total number of averages for that day. Data are grouped in 0.1m intervals from 0-1 m, 0.2 m intervals from 1-3 m and in 0.5m intervals for thicknesses > 3m. B. Cumulative fraction of ice thicknesses on February 3 based on one minute averages, ten minute averages, and hourly averages.

Figure 6. A. Ten minute average thicknesses at station 1 and station 4. B. Ten minute average thickness at station 2 and station 3. C. Tenth percentile data at stations 1, 2, 3, and 4. D. Eightieth percentile data at stations 1, 2, 3, and 4.

Figure 7. A. Hourly burst average thicknesses at stations 4a, 5a, and 6a. B. Tenth percentile thicknesses at stations 4a, 5a, and 6 . C. Eightieth percentile thicknesses at stations 4a, 5a, and 6a.

Figure 8. A. Hourly burst average thicknesses at stations 4 (SWIPS sensor) and 4a (AWACS sensor). B. Tenth percentile thicknesses at stations 4 (SWIPS sensor) and 4a (AWACS sensor). C. Eightieth percentile thicknesses at stations 4 (SWIPS sensor) and 4a (AWACS sensor).

Figure 9. Hourly burst average thicknesses at stations 4 (ASL Environmental Sciences SWIPS sensor, horizontal axis) and 4a (Nortek AWAC sensor, vertical axis).

Figure 10. Ice thicknesses from NIC area J on February 3, 2011. Dotted horizontal lines in each panel are the upper and lower range of NIC ice thicknesses. The time of the MODIS image in Fig. 2 is indicated by the X in each panel. A. Ten minute and hourly average thicknesses at station 1. B. Ten minute and hourly average thicknesses at station 4, and hourly thicknesses at station 4a. Dotted horizontal lines are upper and lower range of NIC ice thicknesses. C. Hourly thicknesses at station 5a,

Figure 11. Ice thicknesses from NIC area G on February 3, 2011. Dotted horizontal lines are upper and lower range of NIC ice thicknesses. The time of the MODIS image in Fig. 2 is indicated by the X in each panel. A. Ten minute and hourly average thicknesses at station 2 B. Ten minute and hourly average thicknesses at station 3. C. Hourly thicknesses at station 6a.

Table 1. Deployment information. All moorings were deployed in 2010 and retrieved in 2011. MAB is meters above bottom.

Station	1	2	3	4	4a	5a	6a	7
Deployed	Oct. 25	Oct. 25	Nov. 3	Nov. 4	Nov. 4	Nov. 4	Nov. 3	Nov. 3
Retrieved	June 16	June 16	June 2	June 15	June 15	June 20	June 2	June 15
Latitude	41.637°	41.776°	42.010°	41.768°	41.767°	41.740°	42.132°	41.944°
Longitude	81.962°	82.084°	82.266°	81.498°	81.501°	81.746°	81.893°	81.642°
Depth	17.9m	19.8m	18.7m	18.6m	18.6m	20.6m	19.0m	23.0m
SWIPS	2-3 mab	2-3 mab	2-3 mab	2-3 mab				
ADCP	0.5 mab	0.5 mab	0.5 mab					0.5 mab
AWAC					0.5 mab	0.5 mab	0.5 mab	
Temp Sensors	1,2,4,6, 8 mab	1,4,6,8, 10 mab	1,3,5,7, 9 mab	1,3,5,7, 9 mab		1, 4,7,9, 11 mab	1,3,5,7, 9 mab	1,4,7,9,11, 13,15 mab
Pressure sensors						1.36 mab	1.37 mab	1.30 mab
Transmiss -ometer						0.85 mab	0.87 mab	0.95 mab

Table 2. Ice thicknesses on February 3, 2011 for 70% and 30% of full ice cover from Naval Ice Center analyses.

NIC area	Area J		Area G	
Concentrations	70%	30%	30 %	70%
Thicknesses	0.15-0.30 m	0.30-0.70 m	0.05-0.15 m	0.15-0.30 m

Table 3. Ice thicknesses on February 3, 2011 from time series measurements. Stations 1, 4, 4a, and 5a are in NIC area J, and stations 2, 3, and 6a are in NIC area G.

Stations	1	4	4a	5a	2	3	6a
Mean	0.26m	0.58m	0.35m	0.47m	0.33m	0.45m	0.42m
10%	0.14m	0.27m	0.16m	0.22m	0.18m	0.15m	0.12m
80%	0.39m	0.88m	0.42m	0.72m	0.39m	0.67m	0.64m

Table 4: Mean differences between NIC and observations

Station	#obs	<=5 cm	5-15 cm	15-30 cm	30-70 cm	Average
1	20	18%	20%	23%	16%	19%
2	23	22%	17%	12%	6%	14%
3	21	26%	30%	4%	1%	15%
4	19	20%	44%	39%	26%	32%
4a	19	3%	22%	27%	20%	18%
5a	21	-11%	-10%	5%	9%	-2%
6a	21	3%	-5%	6%	3%	2%
Average		12%	17%	15%	12%	

Table 5: Standard deviation of mean differences

Station	#obs	<=5 cm	5-15 cm	15-30 cm	30-70 cm
1	20	38%	32%	27%	29%
2	23	37%	43%	28%	9%
3	21	39%	37%	20%	5%
4	19	29%	45%	47%	20%
4a	19	28%	53%	40%	20%
5a	21	23%	30%	32%	15%
6a	21	32%	24%	14%	7%

Table 6. Maximum ice thicknesses (m) based on 1, 10, 17 (burst) minute, hourly, and daily averages.

Station	1 minute	10 minute	Burst	Hourly	Daily
1	10.25	8.30	-	5.34	3.18
2	9.04	5.93	-	3.68	1.33
3	7.37	5.72	-	2.88	0.45
4	9.65	8.31	-	4.81	2.13
4a	5.80	-	4.91	-	1.43
5a	6.27	-	3.82	-	1.26
6a	5.84	-	4.33	-	1.12

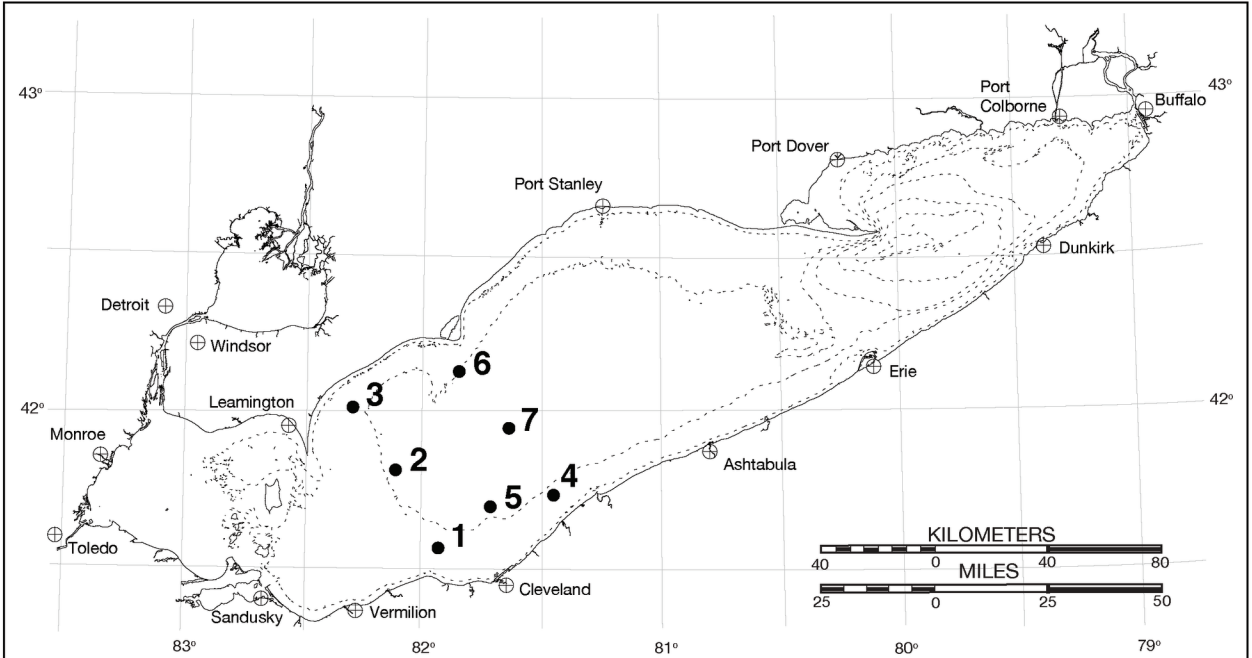
43°
42°
83°
82°
81°
80°
79°
Port Colborne
Buffalo
Port Dover
Port Stanley
Dunkirk
Detroit
Windsor
Leamington
Monroe
Erie
Ashtabula
Toledo
Sandusky
Vermilion
Cleveland
1
2
3
4
5
6
7
KILOMETERS
40 0 40 80
MILES
25 0 25 50


6
3
7
2
4
5
1

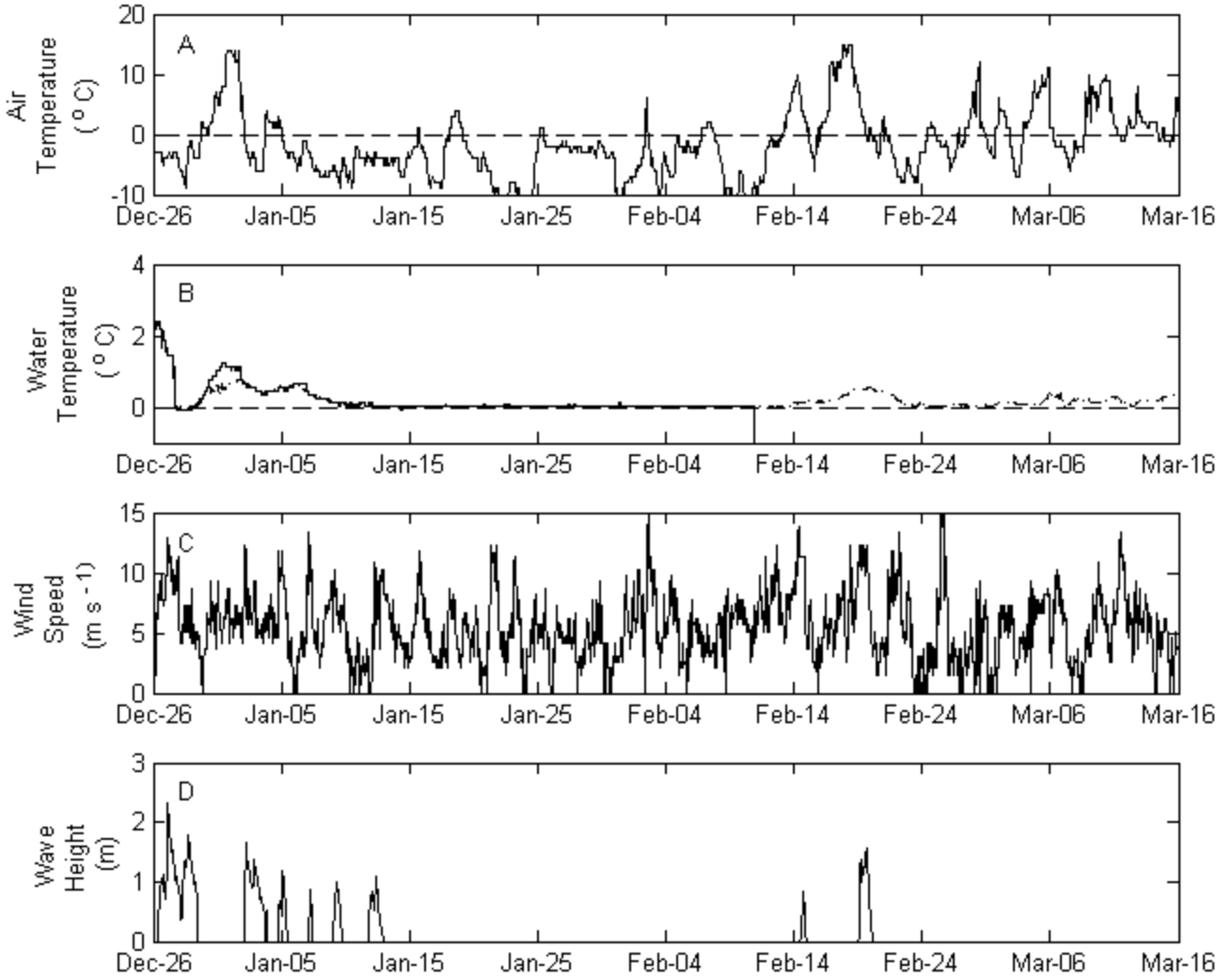
A
Air Temperature (° C)
20
10
0
-10
B
Water Temperature (° C)
4
2
0
C
Wind Speed (m s -1)
15
10
5
0
D
Wave Height (m)
3
2
1
0
Dec-26
Jan-05
Jan-15
Jan-25
Feb-04
Feb-14
Feb-24
Mar-06
Mar-16

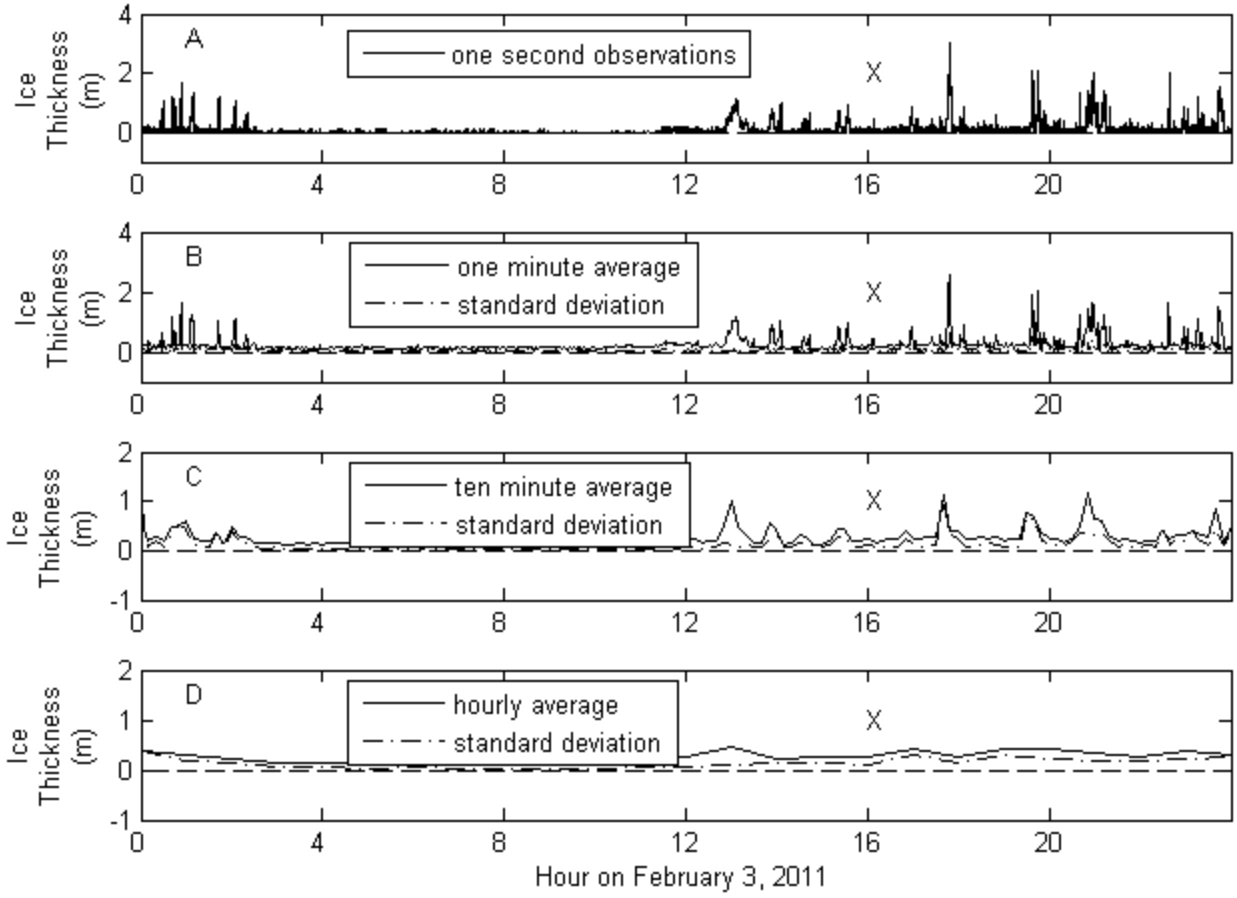
A
one second observations
X
B
one minute average
standard deviation
X
C
ten minute average
standard deviation
X
D
hourly average
standard deviation
X
Ice Thickness (m)
Hour on February 3, 2011

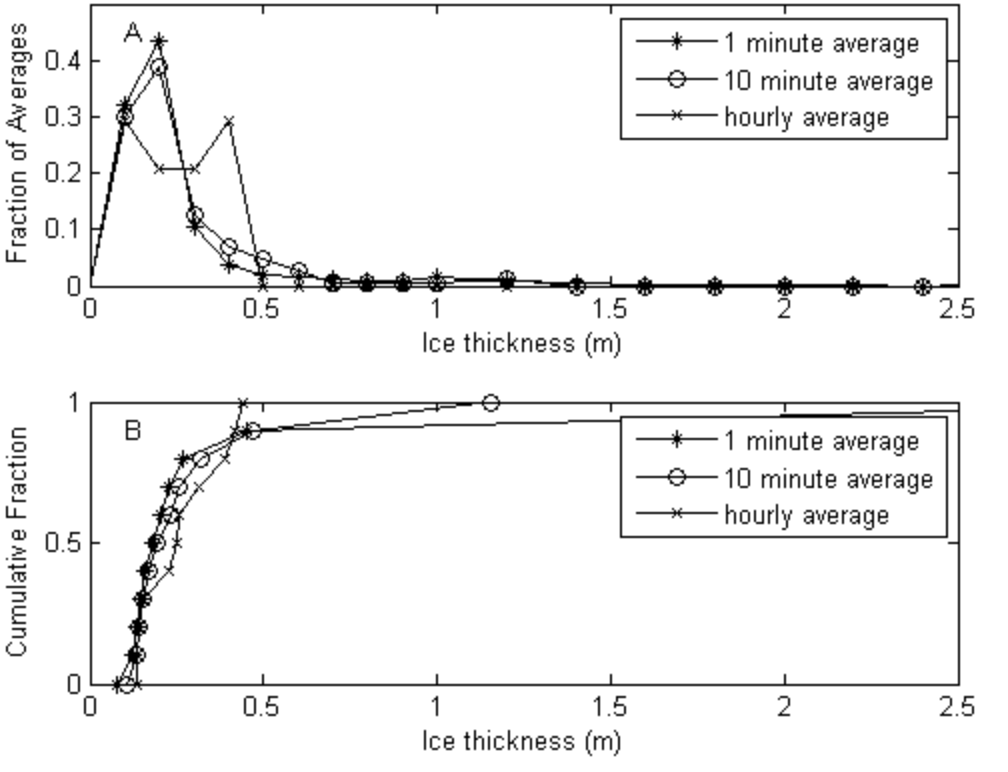
A
Fraction of Averages
0
0.1
0.2
0.3
0.4
0
0.5
1
1.5
2
2.5
Ice thickness (m)
1 minute average
10 minute average
hourly average
B
Cumulative Fraction
0
0.5
1
0
0.5
1
1.5
2
2.5
Ice thickness (m)
1 minute average
10 minute average
hourly average

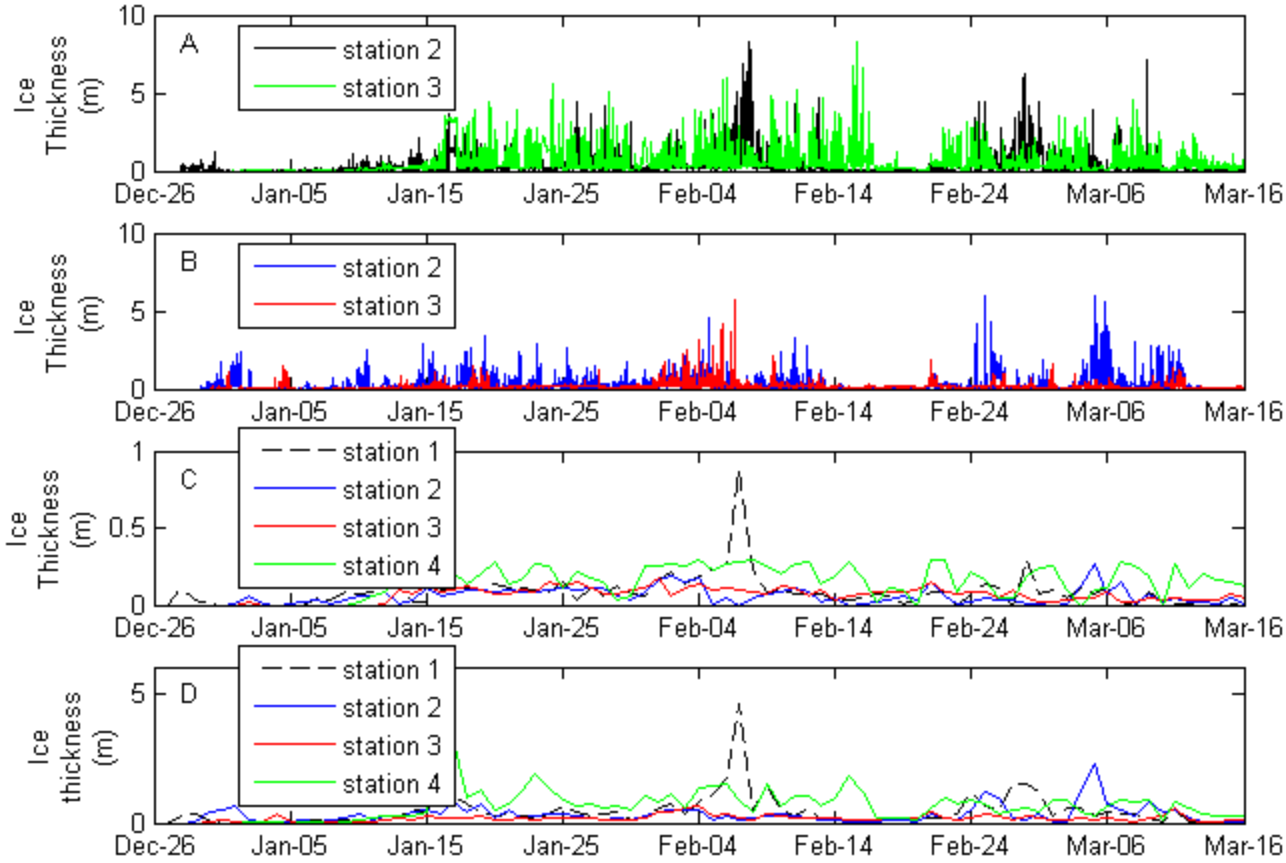
A
station 2
station 3
Ice Thickness (m)
10
5
0
B
station 2
station 3
Ice Thickness (m)
10
5
0
C
station 1
station 2
station 3
station 4
Ice Thickness (m)
1
0.5
0
D
station 1
station 2
station 3
station 4
Ice thickness (m)
5
0
Dec-26
Jan-05
Jan-15
Jan-25
Feb-04
Feb-14
Feb-24
Mar-06
Mar-16

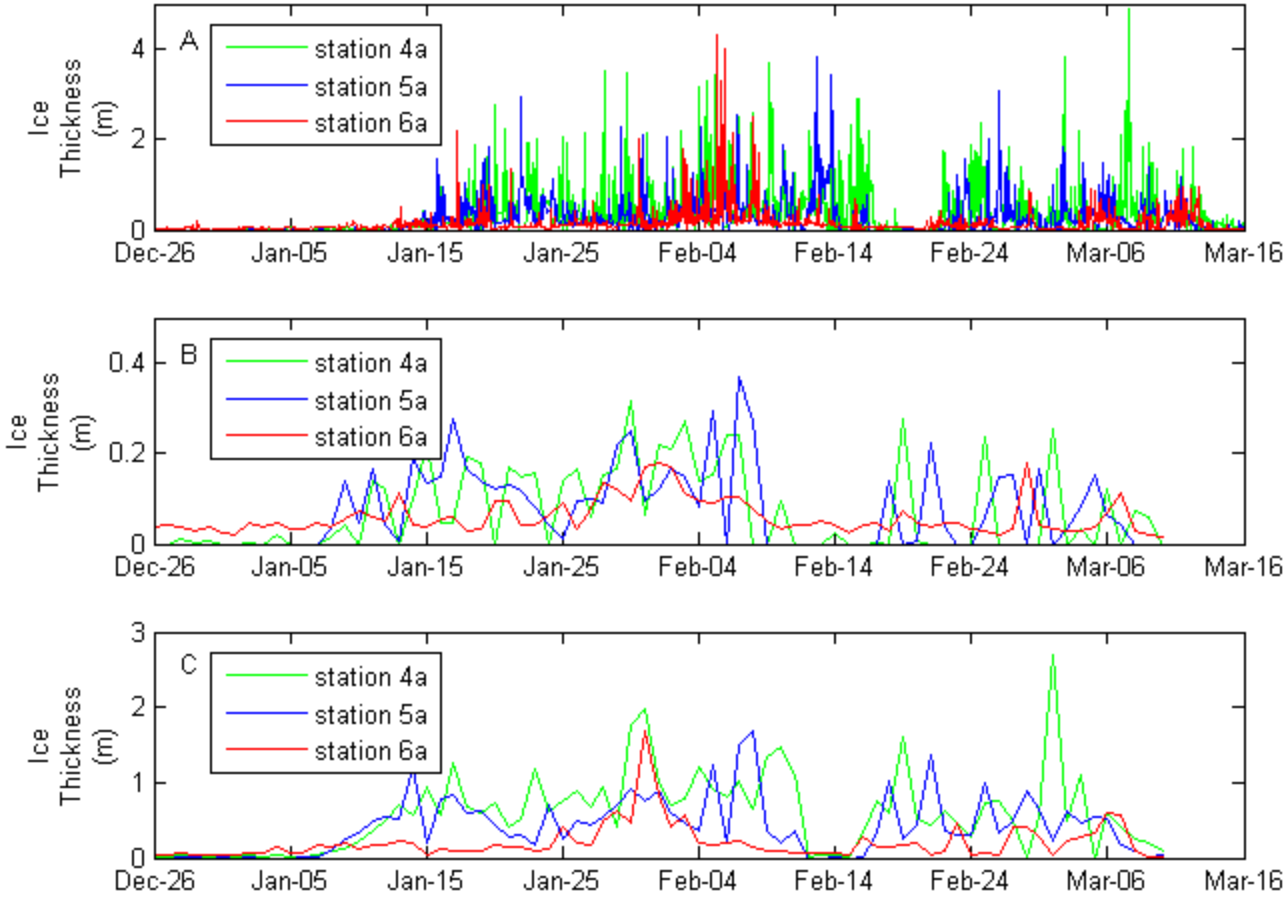
A
station 4a
station 5a
station 6a
Ice Thickness (m)
0
2
4
Dec-26
Jan-05
Jan-15
Jan-25
Feb-04
Feb-14
Feb-24
Mar-06
Mar-16
B
station 4a
station 5a
station 6a
Ice Thickness (m)
0
0.2
0.4
Dec-26
Jan-05
Jan-15
Jan-25
Feb-04
Feb-14
Feb-24
Mar-06
Mar-16
C
station 4a
station 5a
station 6a
Ice Thickness (m)
0
1
2
3
Dec-26
Jan-05
Jan-15
Jan-25
Feb-04
Feb-14
Feb-24
Mar-06
Mar-16

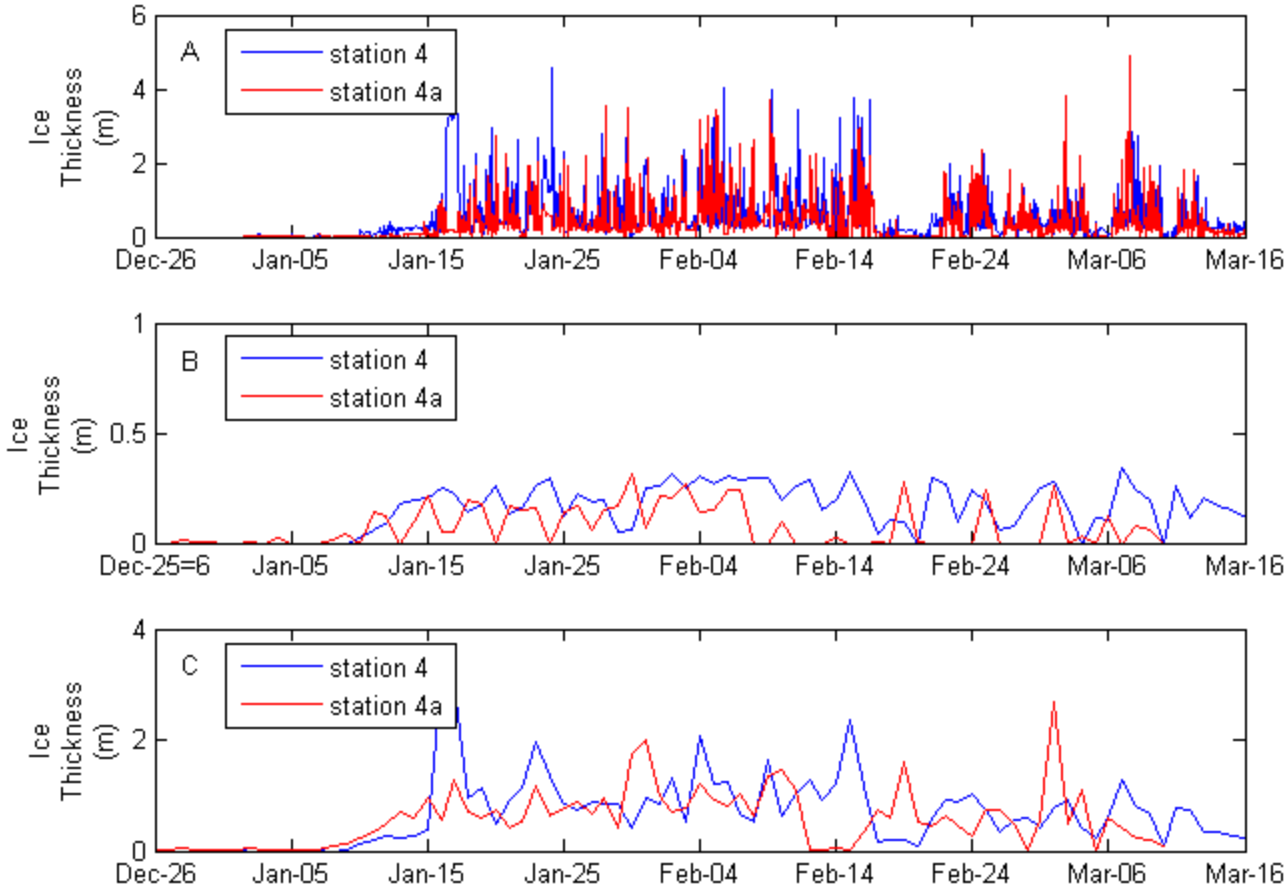
A
station 4
station 4a
Ice Thickness (m)
6
4
2
0
Dec-26
Jan-05
Jan-15
Jan-25
Feb-04
Feb-14
Feb-24
Mar-06
Mar-16
B
station 4
station 4a
Ice Thickness (m)
1
0.5
0
Dec-25=6
Jan-05
Jan-15
Jan-25
Feb-04
Feb-14
Feb-24
Mar-06
Mar-16
C
station 4
station 4a
Ice Thickness (m)
4
2
0
Dec-26
Jan-05
Jan-15
Jan-25
Feb-04
Feb-14
Feb-24
Mar-06
Mar-16

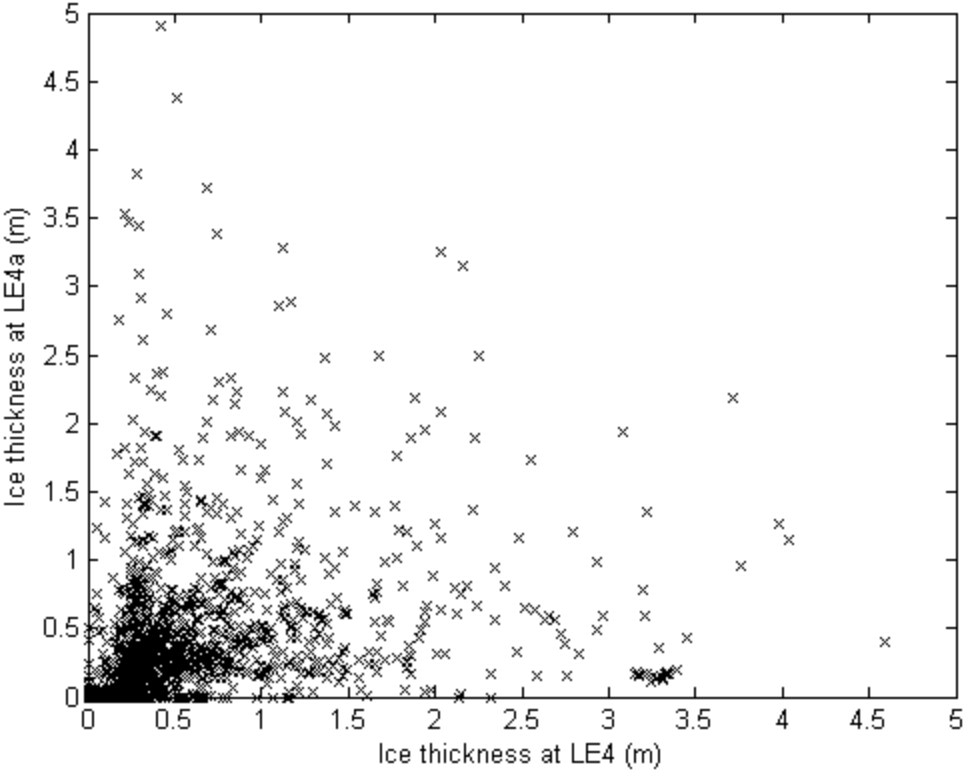
Ice thickness at LE4a (m)
Ice thickness at LE4 (m)
0
0.5
1
1.5
2
2.5
3
3.5
4
4.5
5

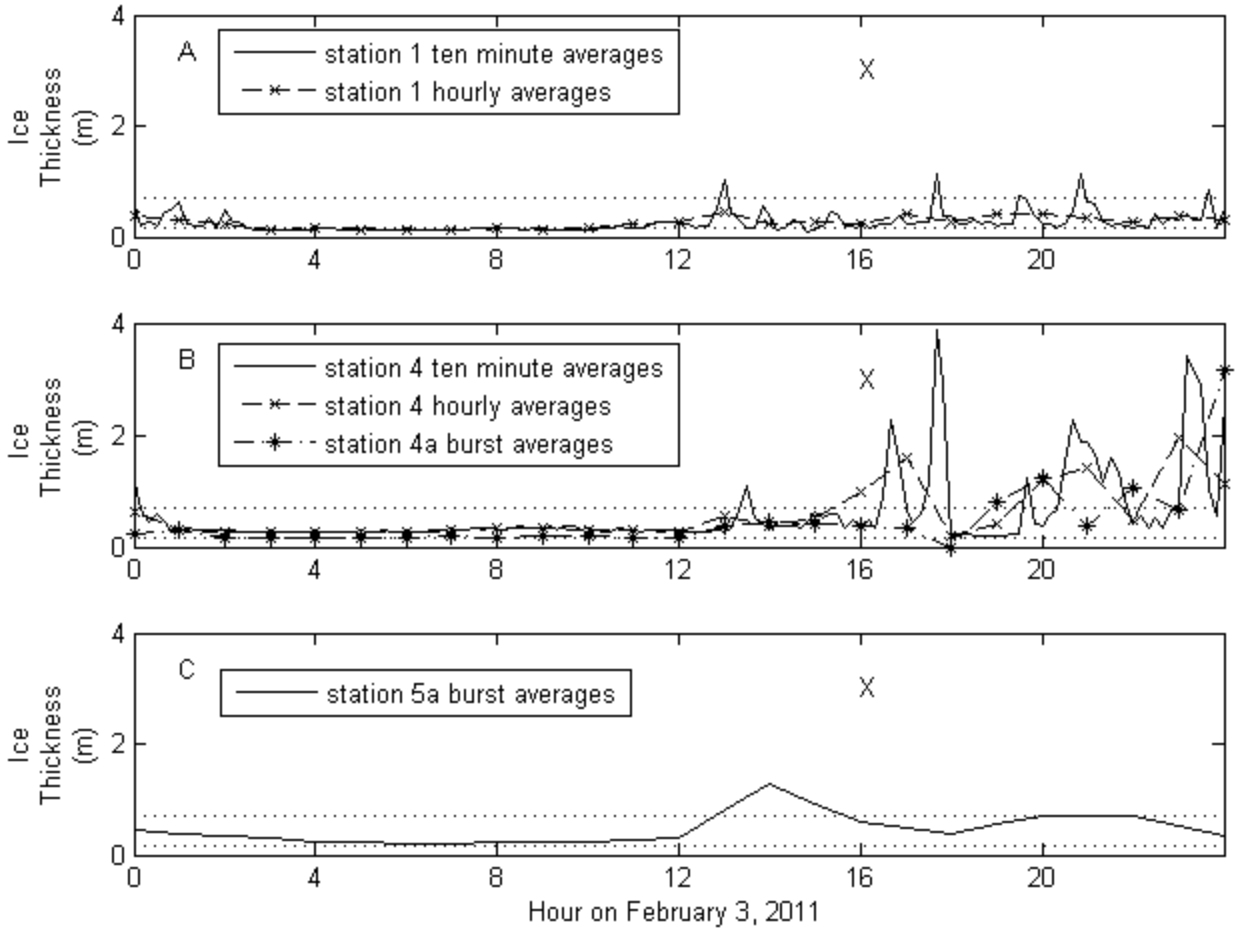
A
station 1 ten minute averages
station 1 hourly averages
X
Ice Thickness (m)
B
station 4 ten minute averages
station 4 hourly averages
station 4a burst averages
X
Ice Thickness (m)
C
station 5a burst averages
X
Ice Thickness (m)
0
2
4
0
4
8
12
16
20
Hour on February 3, 2011

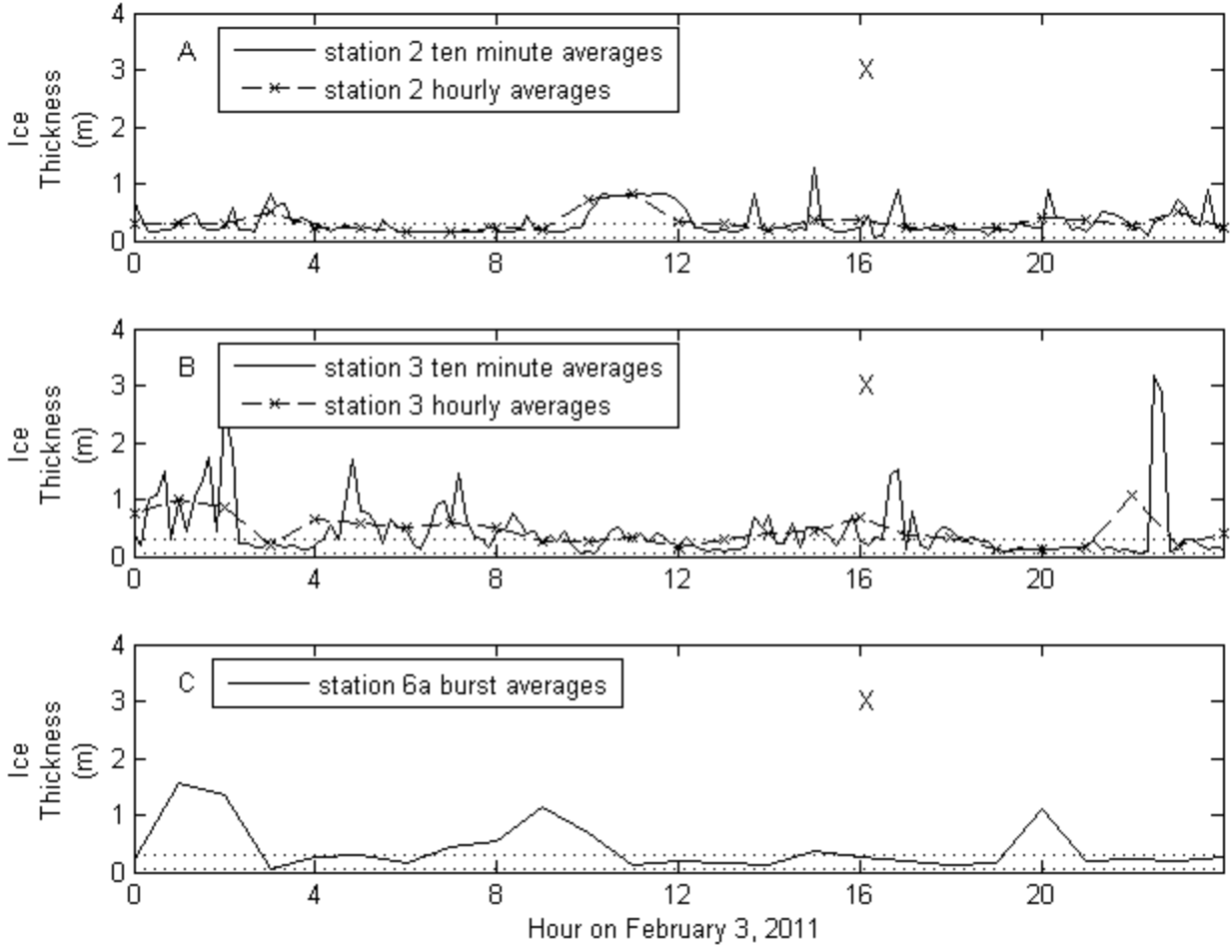
A
station 2 ten minute averages
station 2 hourly averages
X
Ice Thickness (m)
B
station 3 ten minute averages
station 3 hourly averages
X
Ice Thickness (m)
C
station 6a burst averages
X
Ice Thickness (m)
0
1
2
3
4
0
4
8
12
16
20
Hour on February 3, 2011